THE EUROPEAN
PHYSICAL JOURNAL D

Regular Article - Plasma Physics

Application of GK$^1\Sigma_g^+$, $\nu' = 0 \to$ B$^1\Sigma_u^+$, $\nu'' = 0$ hydrogen band for the axial temperature measurement in the cathode sheath region of an abnormal glow discharge

M. M. Vasiljević[1,a], G. LJ. Majstorović[2], DJ. Spasojević[1], and N. Konjević[1]

[1] Faculty of Physics, University of Belgrade, Studentski trg 12, 11000 Belgrade, Serbia
[2] University of Defence, Military Academy, Gen. Pavla Jurišića Šturma 33, 11040 Belgrade, Serbia

Abstract. In this paper, optical emission spectroscopy technique was used to measure rotational and gas temperature distribution in the cathode-sheath region of an abnormal glow discharge operated in hydrogen and hydrogen–argon mixtures. The rotational temperature of excited electronic states of H_2 was determined from the R-branch of the GK$^1\Sigma_g^+$, $\nu' = 0 \to$ B$^1\Sigma_u^+$, $\nu'' = 0$ band and compared with published results for the Q-branch of the Fulcher-α diagonal band d$^3\Pi_u^-$, $\nu' \to$ a$^3\Sigma_g^+$, $\nu''(\nu' = \nu'' = 0)$. The population of excited energy levels, determined from the relative line intensities, was used to derive the rotational temperature of the ground state of hydrogen molecule. The boundary between the cathode sheath and negative glow region is determined using Stark polarization spectroscopy of the hydrogen Balmer alpha line. The thickness of the cathode sheath is estimated by fitting the experimentally determined distribution of electric field strength to a suitable model function. Temperature distributions along the axis of the cathode sheath are also reported and discussed. The distributions of temperature show that both bands give consistent and reasonable values for the rotational temperature and they both mutually agree within the estimated experimental uncertainties of 15%. The reported results contribute to the development of the spectroscopic method for gas temperature measurement in pure molecular hydrogen and in the gas mixture with argon.

1 Introduction

To understand plasma fundamentals, phenomena and applications, it is required to know the values of discharge parameters (e.g., the electric field strength distribution, gas and vibrational temperatures of molecules and radicals) primarily in the cathode sheath (CS) region of discharge. This region is the most important part of abnormal glow discharge (GD) since most of the relevant processes for the operation and application of GD occur in CS. Therefore, this region of discharge has been a subject of numerous experimental and theoretical studies [1–18], and its importance cannot be neglected when describing or modelling GD.

The most important parameter of the CS region is the electric field strength distribution, which depends on current density, pressure, cathode material, geometry of the discharge, etc., and determines the acceleration of the charged particles, influencing their path and kinetic energy. In addition, gas (translational) temperature T_g is of great importance since it determines the rate of chemical reactions.

The Fulcher-α band is very convenient and commonly used for measurement of the gas temperature because the lines are located in the visible region of spectrum. In addition, the upper-level energies and wavelengths for most of the hydrogen bands are not described by standard formulae due to perturbations from nearby energy levels. It is known that d$^3\Pi_u$ state degenerates into the d$^3\Pi_u^+$ and d$^3\Pi_u^-$ state due to the Λ-type doubling [19]. The d$^3\Pi_u^-$ state has only a Q-branch, while the d$^3\Pi_u^+$ has P- and R-branches in the spontaneous ro-vibrational emission to a$^3\Sigma_g^+$. The degenerate d$^3\Pi_u^+$ state interacts strongly with the e$^3\Sigma_u^+$ state, so the P- and R-branches of Fulcher-α are perturbed. Encouraged by this fact, we used so far only the Q-branches of the Fulcher-α hydrogen band for the temperature measurement in the CS region of abnormal GD [18] rather than any other molecular system.

It is shown in the literature [20–22], however, that it is also possible to use the $\nu' = \nu'' = 0$ band in the GK$^1\Sigma_g^+$, $\nu' \to$ B$^1\Sigma_u^+$, ν'' electronic transition for temperature determination despite that this transition is more complicated to handle since its upper electronic level is a complex state consisting of two electronic states, $(1s\sigma 3d\sigma)^1\Sigma_g^+$ and doubly excited state $(2p\sigma^2)^1\Sigma_g^+$. The state GK$^1\Sigma_g^+$ has double min-

a e-mail: milica.vasiljevic@ff.bg.ac.rs (corresponding author)

ima potential curve [23] and represents an intermediate case between two limiting Hund's cases b and d [24]. Furthermore, $GK^1\Sigma_g^+$ electronic state is perturbed by an electronic-rotation coupling with several electronic states $EF^1\Sigma_g^+$, $HH^1\Sigma_g^+$, $I^1\Pi_g^+$, $J^1\Delta_g^+$ [20] and references therein.

Since the electronic transition $GK^1\Sigma_g^+ \rightarrow B^1\Sigma_u^+$ is of the $^1\Sigma \rightarrow {}^1\Sigma$ type, the Q-branch does not exist. In several publications, it was proposed to use the line intensities within the R-branch of the $\nu' = \nu'' = 0$ band in $GK^1\Sigma_g^+$, $\nu' \rightarrow B^1\Sigma_u^+$, ν'' electronic transition for temperature measurement in hydrogen low-pressure gas discharges [22–24]. The temperature obtained using a limited number of spectral lines from the R-branch of $GK^1\Sigma_g^+ \rightarrow B^1\Sigma_u^+$ transition agrees well with the temperature measured from the Q-branch of Fulcher-α band [20].

The $GK^1\Sigma_g^+$, $\nu' \rightarrow B^1\Sigma_u^+$, $\nu''(\nu' = \nu'' = 0)$ band is located in the wavelength region where most of radiation detectors have a high sensitivity, which makes these lines very attractive candidates for various applications. Spectral lines belonging to this band are very intensive and well resolved, so their identification is not complicated. The aim of this study is to investigate the possibility of using the $GK^1\Sigma_g^+$, $\nu' \rightarrow B^1\Sigma_u^+$, ν'' band for temperature determination within the cathode sheath region of an abnormal discharge. To this end, we present experimental results of the temperature distributions and compare them with rotational and gas spectroscopic temperature measurements using $GK^1\Sigma_g^+$, $\nu' \rightarrow B^1\Sigma_u^+$, ν'' and Fulcher-α band. The boundary of the cathode sheath is determined using the well-established techniques for evaluation of the electric field strength distribution, previously described in [12,13,25]. In this study, through CS region of an abnormal glow discharge operated at low pressure of hydrogen or in the hydrogen–argon gas mixture, the Fulcher-α diagonal and $GK^1\Sigma_g^+$, $\nu' \rightarrow B^1\Sigma_u^+$, ν'' bands are recorded, results analyzed and temperatures derived and compared, using optical emission spectroscopy (OES) technique. The gas mixture was used to check the influence of a small admixture of argon in hydrogen to the thickness of CS region, line intensities and resolution of the spectral bands.

2 Experimental

A plane cathode–hollow anode glow discharge source (GDS) used for experiments was laboratory-made according to the Grimm-type GDS modified by Fereira et al. [6] and Kuraica et al. [26]. A hollow 30-mm-long anode with inner diameter of 8 mm has a 1.5 mm wide longitudinal slot for side-on observations along the discharge axis, see Fig. 1. To the water-cooled cathode holder is attached an exchangeable copper electrode, 18 mm long and 7.60 mm in diameter, which is screwed tightly into its holder to ensure good cooling. The gas flow of about $300\,\text{cm}^3\,\text{min}^{-1}$ of pure hydrogen gas (vol. 99.999%) and
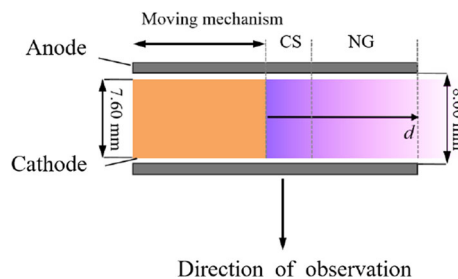

Fig. 1 Schematic diagram of the central part of our GDS, where CS denotes the cathode sheath region, NG—negative glow region, and d—distance from the cathode

hydrogen–argon mixture (95% H_2 and 5%Ar) is kept at a pressure about 5 mbar by means of a needle valve and two two-stage mechanical vacuum pumps. The gas pressure was evaluated as the average value between the gas inlet and outlet measured values.

A current stabilized power supply (0 kV–2 kV, 0 mA–100 mA) was used to run the discharge. For all experiments, a 5.3 kΩ ballast resistor was placed in series with the discharge and power supply.

Spectroscopic recordings of GD were performed side-on through the anode slot in translation steps of approximately 1/16 mm for the hydrogen Balmer-α line and in steps of 1/8 mm for the Fulcher-α and $GK^1\Sigma_g^+$, $\nu' \rightarrow B^1\Sigma_u^+$, ν'' band lines. When the Stark polarization spectroscopy is applied, a plastic polarizer was used.

Spectroscopic measurements were performed with 2 m focal length Ebert-type spectrometer with 651 grooves/mm reflection grating blazed at 1050 nm. The reciprocal dispersion of reflection grating in the second diffraction order is 0.37 nm/mm with instrumental profile very close to the Gaussian form with measured full width at half maximum (FWHM) ~0.014 nm. All spectroscopic data were collected with a thermoelectrically cooled Hamamatsu CCD (2048 × 506 pixels, pixel size $12 \times 12\,\mu\text{m}$, $-10°\text{C}$) Consequently, the data were transferred to and processed by a PC. The wavelength sensitivity calibration of the spectrometer–radiation detector system was done by using the standard tungsten lamp.

3 Results and discussion

3.1 Determination of the electric field strength distribution

Spectroscopic side-on measurements of electric field strength have to be performed with line radiation collected only from discharge regions with the electric field considered as homogeneous. In the side-on measurements, performed in the CS region of glow discharges with plane cathode, this condition is approximately satisfied for the radiation collected from a narrow cylindrical region of discharge parallel to the cathode surface

because in the thin ($\sim 1\,\mathrm{mm}$) cathode region of such discharges the electric field strength vectors are practically perpendicular to the cathode surface and their magnitude F depends almost only on the distance to the cathode surface. It is known that spectral lines of atomic hydrogen exhibit linear Stark effect [2], so the knowledge of the Stark shift coefficients for a certain type of polarized spectral line enables one to perform the spectroscopic measurement of electric field strength F from the shape of the recorded line profile.

One of the techniques for measuring the electric field strength is by using spectral line shape of atomic hydrogen, here the π- polarized H_α line, and establish a suitable model function for the profile shape depending on the electric field strength F as parameter adjusted so as to achieve the best matching between the model profile and the recorded line profile.

For the estimation of the CS region thickness, we employ the same technique previously described in [18]. The electric field strength distribution is determined by fitting the experimentally obtained profiles of the π-polarized hydrogen Balmer H_α line with the model function (1):

$$
\begin{aligned}
I(\Delta\lambda; F) = b + \Im * \{ & G(\Delta\lambda; H_1, c_1, w_1) \\
& + G(\Delta\lambda; H_2, c_2, w_2) \\
& + G(\Delta\lambda; H_3, c_3, w_3, w_3) \\
& + S_F * [G(\Delta\lambda; zH_1, c_1, w_1) \\
& + G(\Delta\lambda; zH_2, c_2, w_2) \\
& + G(\Delta\lambda; zH_3, c_3, w_{L3}, w_3)] \}
\end{aligned} \tag{1}
$$

The model function (1) together with the best fit and all the parameters are explained in details in [18]. Using the previously reported technique in [18], we determined that the thickness of the CS region does not exceed 2.25 mm, in pure hydrogen discharge, while for the hydrogen–argon discharge, the thickness is 1.75 mm. The knowledge of this value is essential for the further analysis, since we want to show the variations of the rotational and gas temperature, T_{rot} and T through the CS region.

3.2 Molecular spectra recording

In Fig. 2, we present recorded rotational bands of the Fulcher-α diagonal band ($\nu' = 0$) and the $\mathrm{GK}^1\Sigma_g^+$, $\nu' \to \mathrm{B}^1\Sigma_u^+$, ν'' band in hydrogen and hydrogen–argon mixture. Therefrom, it is evident that the Q-branch lines of the electronic transition $\mathrm{d}^3\Pi_\mathrm{u}^-$, $\nu' \to \mathrm{a}^3\Sigma_\mathrm{g}^+$, $\nu''(\nu' = \nu'' = 0)$, as well as the R-branch lines of the $\mathrm{GK}^1\Sigma_g^+$, $\nu' \to \mathrm{B}^1\Sigma_u^+$, $\nu''(\nu' = \nu'' = 0)$, are well resolved and intensive. The $\mathrm{GK}^1\Sigma_g^+$, $\nu' \to \mathrm{B}^1\Sigma_u^+$, $\nu''(\nu' = \nu'' = 0)$ band is located in the wavelength region (wavelength data taken from [27]) where most of radiation detectors have a high sensitivity, see, e.g., [18], which makes these lines very attractive candidates for various applications. Although intensities of P-branch lines are weaker for almost two orders

of magnitude than those from R-branch of the same electronic-vibrational transition, the spectral resolution and signal-to-noise ratio of our spectrometer–detector system enabled their identification.

3.2.1 Results and discussion

In previous studies of hollow cathode glow discharge (HCGD), see [20,28], it was shown that for estimation of the rotational and ground state T_0 temperature, it is feasible to use the first five lines of R-branch of the $\mathrm{GK}^1\Sigma_g^+$, $\nu' \to \mathrm{B}^1\Sigma_u^+$, ν'', $\nu' = \nu'' = 0$ band. Using this knowledge, we test the possibility to use R-branch of $\mathrm{GK}^1\Sigma_g^+$, $0 \to \mathrm{B}^1\Sigma_u^+$, 0 in the cathode sheath region of an abnormal Grimm glow discharge. Rotational and gas temperatures are determined and compared with results obtained from the Q-branch of Fulcher-α band of the same discharge [18].

The recorded rotational bands of the $\mathrm{d}^3\Pi_\mathrm{u}^- \to \mathrm{a}^3\Sigma_\mathrm{g}^+$ and $\mathrm{GK}^1\Sigma_g^+, 0 \to \mathrm{B}^1\Sigma_u^+$, 0 intensity of hydrogen transitions are used for evaluation of the rotational temperature $T_{rot}(n', \nu')$ of the excited state. Here, we use the Boltzmann plot technique based on the experience that the logarithm of the intensity of the spectral line emitted in transition (n, ν', $J' \to n''$, ν'', J'') is a linear function of the upper-level energy. By plotting $\ln\left(\frac{I_{n'',\nu'',J''}^{n',\nu',J'}}{v^4\,g_{a.s.}\,H_{J'J''}}\right)$ against term values for the upper level in the case of Boltzmann population distribution, a straight line with the slope $\frac{h\,c}{k\,T_{rot}(n',\nu')}$ should be obtained [28]; here, v is the wavenumber, $g_{a.s.}$ is the statistical weight of the n',ν', J' rotational level caused by the nuclear spin and the symmetry with respect to the permutation of the nuclei ('a' or 's'), $H_{J'J''}$ are the Hönl–London factors (HL), see [21,29], and $I_{\mathrm{a.u.}} = I_{n'',\nu'',N''}^{n',\nu',N'}C$ is the line intensity where C is a constant factor of proportionality. For molecular hydrogen $g_{a.s.} = g_{s.} = 1$ for even and $g_{a.s.} = g_{a.} = 3$ for odd values of the rotational quantum number J, see, e.g., [20,30], and for the $\Pi \to \Sigma$ electronic transition the factor $H_{J'J''}$ may be written as: (J'' -1) for P-branch, ($2J'' + 1$) for Q-branch and ($J'' + 2$) for R-branch [29,30]. For R- and P-branch of the $^1\Sigma \to {}^1\Sigma$ electronic transition, HL values are J' and ($J' + 1$), respectively, see [31]. The above-mentioned slope of these lines may be used for determination of the excited state rotational temperature $T_{rot}(n', \nu')$, see Fig. 3a, and to check experimentally the validity of the assumed Boltzmann distribution of the population of the rotational levels.

The rotational temperature of excited states is determined from the Q-branch for excited vibrational level $\nu' = 0$ of $\mathrm{d}^3\Pi_\mathrm{u}^-$ and R-branch for excited vibrational level $\nu' = 0$ of $\mathrm{GK}^1\Sigma_g^+ \to \mathrm{B}^1\Sigma_u^+$. The results for different positions along the axis of CS region are presented in the lower part of Fig. 4a for discharge in pure hydrogen, and in the lower part of Fig. 4b for discharge in the hydrogen–argon mixture.
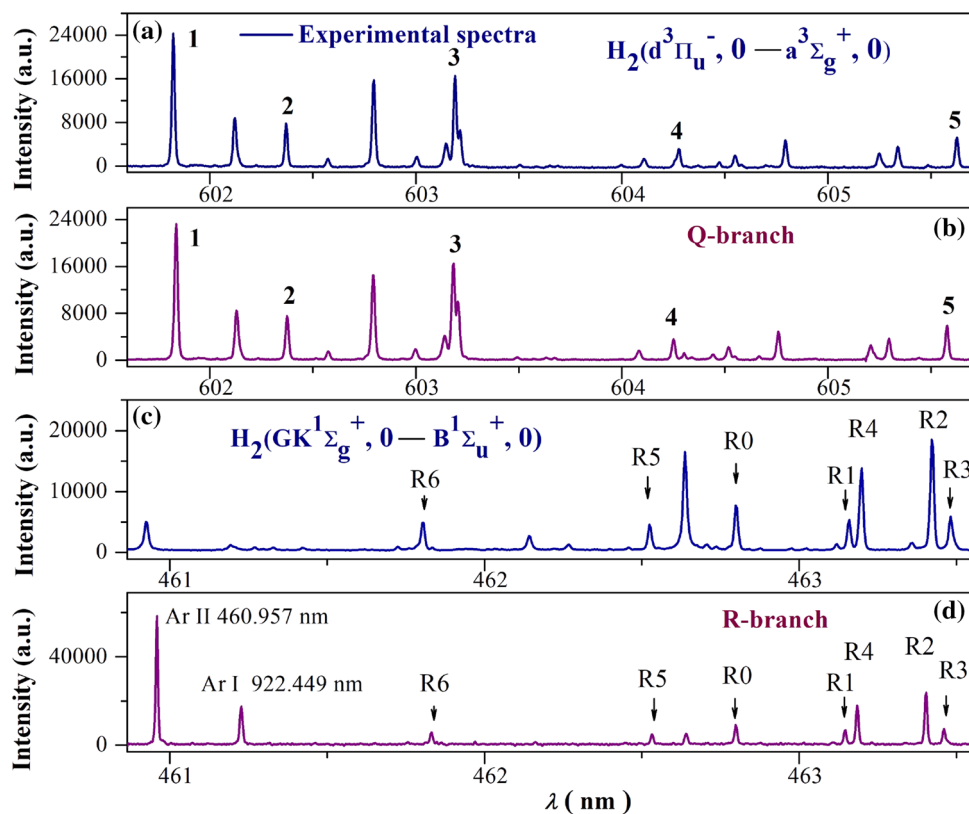
Fig. 2 Emission spectra of the rotational lines for the $d^3\Pi_u^- \rightarrow a^3\Sigma_g^+$ system; **a** and **b** Q-branch (with $\nu' = \nu'' = 0$) and **c** and **d** $GK^1\Sigma_g^+ \rightarrow B^1\Sigma_u^+$ system; R-branch with $\Delta\nu = 0$, $\nu' = 0$ is recorded in the second diffraction order. Experimental conditions: **a** and **c**: discharge in pure H_2 at $p = 4.5$mbar,$I = 11$ mA, and $U = 889$ V **b** and **d**: discharge in $H_2+5\%$Ar at $p = 4.5$mbar, $I = 12$ mA, and$U = 775$ V
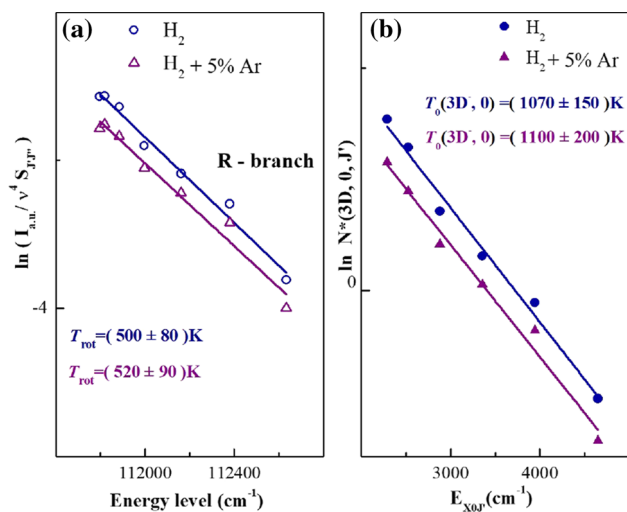

Fig. 3 a Semi-logarithmic plot of the population densities for ro-vibronic levels of H_2 calculated from the measured intensities using the Hönl–London factors. **b** Semi-logarithmic plot of rotational population densities of $GK^1\Sigma_g^+$, 0 versus rotational energy of the molecular hydrogen ground state ($X^1\Sigma_g^+$, $\nu = 0$). Experimental conditions as in Fig. 2

In low-pressure hydrogen discharges, due to small collision frequencies lower than the radiative decay frequencies of the excited state, the number of collisions is not sufficient to redistribute the rotational population as discussed in [32–38] and in references therein. The lifetime values for ro-vibrational levels of electronic state $d^3\Pi_u^-$ and $GK^1\Sigma_g^+$ of the H_2 molecule, given in [37], have been used to calculate radiative decay of these states. Obtained values are $2.5 \cdot 10^7 s^{-1}$ and $4 \cdot 10^7 s^{-1}$, respectively, while in our experimental conditions calculated value for the collision frequency is $2.7 \cdot 10^7 s^{-1}$. On the other hand, the pressure higher than 10 mbar provides collision frequency larger than the radiative decay, which is sufficient to ensure equilibrium of the rotational distribution of this state with the gas temperature [34,35]. In our case, the relation between the population distributions in the excited states and gas temperature should be derived from the balance equations [38]. The model discussed in [17] suggests that the logarithm of the scaled ro-vibrational population density should behave as a linear function of the rotational

energy in the ground $X^1\Sigma_g^+$, $\nu = 0$ vibrational state:

$$\ln N_{n'\nu'J'}^* \equiv \ln \frac{N_{n'\nu'J'}}{g_{a.s.}(2J'+1)\tau_{n'\nu'J'}}$$
$$= -\frac{h\,c\,E_{X0J}}{k\,T_0(n',\nu')} + const, \qquad (2)$$

where $N_{n'\nu'J'}^*$ denote the scaled ro-vibrational population density, while $\tau_{n'\nu'J'}$ is the radiative lifetime of the n',ν', J' level, and E_{X0J} present the ro-vibrational term value of the ground vibrational state. In that case, $T_0(n',\nu')$ represents the rotational temperature of ground vibrational state and can be determined from the rotational population density distribution in an excited (n',ν') vibrational state. This temperature can be also considered as a valid estimation for the ground state ro-vibrational temperature, i.e., H_2 gas temperature, according to [17].

Described model assumes Boltzmann distribution in excited electronic-vibrational states, but one can make an additional assumption and hypothesis that the rotational energy term is $F_N \propto B_{n\nu}J(J+1)$. In this case, the relation between the rotational temperatures in the ground and electronically excited becomes:

$$\frac{T_0(n',\nu')}{B_{X0}} = \frac{T_{rot}(n',\nu')}{B_{n'\nu'}} \qquad (3)$$

where $B_{n'\nu'}$ and B_{X0} are rotational constants of excited states $d^3\Pi_u(30.364\,cm^{-1})$ and $G^1\Sigma_g^+(28.4\,cm^{-1})$ and ground $X^1\Sigma_g^+(60.853\,cm^{-1})$ $(\nu = 0)$ state [21,35].

Thus, the values of the rotational temperature, derived from the population of Q-branch of $d^3\Pi_u^- \to a^3\Sigma_g^+$ or R-branch of $GK^1\Sigma_g^+ \to B^1\Sigma_u^+$ vibrational states $\nu' = 0$, were recalculated to determine the temperature T_0 of the ground vibrational state $X^1\Sigma_g^+(\nu = 0)$ at different positions, see Fig. 3b and the upper part of Fig. 4. The rotational energies $E_{X0J'}$ of the ground $X^1\Sigma_g^+(\nu = 0)$ vibrational state of H_2 were calculated using data listed in [21]. The results obtained for the rotational temperature distribution along the CS region, presented in Fig. 4, show that both temperatures, T_0 and T_{rot} (Q-branch $d^3\Pi_u^-$,0 $\to a^3\Sigma_g^+$, 0 and R-branch $GK^1\Sigma_g^+$, 0 $\to B^1\Sigma_u^+$,0), vary along the CS region and agree within the estimated experimental uncertainties of 15%, which is in good agreement with the uncertainty estimated in [17]. The difference starts to increase as we start to approach the negative glow region.

In our case, the temperature recalculated from (2) for the ground vibrational state $X^1\Sigma_g^+(\nu = 0)$ is almost two times larger than the rotational temperature of excited states $d^3\Pi_u^-$,0 and $GK^1\Sigma_g^+$,0, which is in agreement with (3) because of rotational constants values listed above.

Regarding the temperature vs distance data, shown in Fig. 4 with estimated relative uncertainty of 15% at all points. Possible cause for the temperature variation could be as follows: in low pressure plasmas atoms and
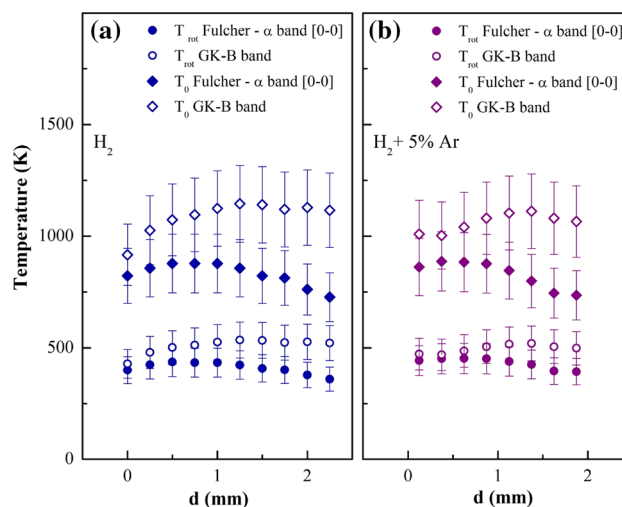

Fig. 4 The dependence of rotational temperature and gas temperature T_0 upon distance from cathode. The values of the rotational and gas temperature for Fulcher-α band taken from [18]. Experimental conditions: copper cathode Grimm GDS **a** in H_2 at $p = 4.5\,mbar$, $I = 11\,mA$, $U = 889\,V$, and the thickness of the CS region less than 2.17 mm; **b** in H_2+5%Ar at $p = 4.5\,mbar$, $I = 12\,mA$, $U = 775\,V$, and the thickness of the CS region less than 1.75 mm

molecules are dominantly excited by electron impact. Following the same pattern, the cross sections for excitation of the $a^3\Sigma_g^+$ and $d^3\Pi_u^-$ levels rapidly decrease with the increase in electron energy above 20 eV [39,40] The cross section for $B^1\Sigma_u^+$ level increases for the energies up to 50 eV and slowly decreases for higher electron energies [39], whereas the cross sections for the corresponding upper level $GK^1\Sigma_g^+$ are not reported in the literature to the authors' knowledge. Assuming that it shows similar dependence on electron energy, one might conjecture that these dependences influence the shape of temperature distributions, reflecting the variation of the average electron energy throughout the cathode sheath, c.f. Fig. 2.38 in [41].

4 Summary and conclusion

The aim of this study is to test the possibility of using the $GK^1\Sigma_g^+$, $\nu' \to B^1\Sigma_u^+$, ν'' band for temperature determination within the cathode sheath region of an abnormal Grimm glow discharge. The $GK^1\Sigma_g^+$, $\nu' \to B^1\Sigma_u^+$, $\nu''(\nu' = \nu'' = 0)$ band is very convenient because it is located in the wavelength region (461–464 nm) where most of radiation detectors have a high sensitivity. This makes these lines very attractive candidates for various applications; also, the spectral lines of this band are very intensive, well resolved and easy for identification.

We used the experience that it is possible to use the first five lines of R-branch of $GK^1\Sigma_g^+ \to B^1\Sigma_u^+$, $\nu' = \nu'' = 0$ band for the measurements of rotational and

ground state T_0 temperature [20,28]. In order to verify the acquired results, we compared them with the corresponding results obtained from the Fulcher-α diagonal band in [18].

To determine the boundary between the CS and the NG region, it was necessary to measure the electric field strength distribution. For the electric field measurement in the cathode sheath region, Stark polarization spectroscopy of hydrogen Balmer alpha line is employed and the thickness of CS region is estimated by fitting the experimentally obtained distribution of electric field strength to a suitable model function reported in [18].

We have recorded and analyzed the electronic transition $GK^1\Sigma_g^+$, $\nu' \rightarrow B^1\Sigma_u^+$, ν'' within the CS region of a hydrogen and hydrogen–argon abnormal glow discharge at low pressure. The axial distribution of rotational temperatures is determined using the Boltzmann plot technique.

The values of the rotational temperature derived from the population of R-branch of $GK^1\Sigma_g^+ \rightarrow B^1\Sigma_u^+$ vibrational states $\nu\prime = 0$ were recalculated to determine the temperature T_0 of the ground vibrational state $X^1\Sigma_g^+(\nu = 0)$) at different positions along CS and compared with already reported results [18] from Q-branch of $d^3\Pi_u^- \rightarrow a^3\Sigma_g^+$. The temperature recalculated for the ground state $X^1\Sigma_g^+$ ($\nu = 0$), see [16], is approximately two times larger than the rotational temperature of excited states. This result corresponds to the ratio of the rotational constants of excited state.

Presented results show that the temperatures (rotational and gas) vary along the CS region of the discharge. The temperatures of both bands, Fulcher-α and $GK^1\Sigma_g^+ \rightarrow B^1\Sigma_u^+$ give consistent and reasonable values and mutually agree within the experimental uncertainty of 15%. In the negative glow region, the uncertainty starts to increase. With this in mind, we could employ R-branch of $GK^1\Sigma_g^+ \rightarrow B^1\Sigma_u^+, \nu' = \nu'' = 0$ band for quick measurement of rotational and ground state T_0 temperature within the CS region of the Grimm glow discharge.

Data Availability Statement This manuscript has no associated data, or the data will not be deposited. [Authors' comment: All the data are shown in the paper.].

References

1. N. Jakubowski, A. Bogaerts, V. Hoffmann, Atomic Spectroscopy in Elemental Analysis, in *Glow discharges in emission and mass spectrometry*, ed. by M. Cullen (Blackwell Publishing, Sheffield, 2003)
2. J.A.C. Broekaert, *Glow Discharge Plasmas in Analytical Spectroscopy* (Wiley, New York, 2003)
3. W. Grimm, Spectrochim. Acta B **23**, 443 (1968)
4. G.L. Majstorović, N.V. Ivanović, N.M. Šišović, S. Djurović, N. Konjević, Plasma Sour. Sci. Technol. **22**, 045015 (2013)
5. W. Grimm, Naturwissenschaften **54**, 586 (1967)
6. N.P. Ferreira, H.G.C. Human, L.R.P. Butler, Spectrochim. Acta B **35**, 287 (1980)
7. A. von Engel, *In Ionized Gases* (Clarendon Press, Oxford, 1965)
8. B. Chapman, *In glow discharge processes sputtering and plasma etching* (Wiley, New York, 1980)
9. D. Spasojević, V. Steflekova, N.M. Šišović, N. Konjević, Plasma Sour. Sci. Technol. **21**, 025006 (2012)
10. C. Biloiu, X. Sun, Z. Harvey, E. Scime, Rev. Sci. Instr. **77**, 10F117 (2006)
11. E.M. Hollmann, A.Y. Pigarov, K. Taylor, J. Nucl. Mater. **337**–**339**, 451 (2005)
12. N.V. Ivanović, N.M. Šišović, D. Spasojevć, N. Konjević, J. Phys. D Appl. Phys. **50**, 125201 (2017)
13. D. Spasojević, V. Steflekova, N.M. Šišović, N. Konjević, Plasma Sour. Sci. Technol. **23**, 12004 (2014)
14. M.M. Vasiljević, D. Spasojević, N.M. Šišović, N. Konjević, Europhys. Lett. **119**, 55001 (2017)
15. H. Tawara, Y. Itikawa, H. Nishimura, M. Yoshino, J. Phys. Chem. **19**, 617 (1990)
16. G.L. Majstorović, N.M. Šišović, N. Konjević, Plasma Sour. Sci. Technol. **16**, 750 (2007)
17. S.A. Astashkevich, M. Käning, E. Käning, N.V. Kokina, B.P. Lavrov, A. Ohl, J. Röpcke, J. Quant. Spectrosc. Radiat. Transf. **56**, 725 (1996)
18. M.M. Vasiljević, G.L. Majstorović, D. Spasojević, N. Konjević, J. Quant. Spectrosc. Radiat. Transf. **254**, 107195 (2020)
19. B. Xiao, S. Kado, S. Kajita, D. Yamasaki, Plasma Phys. Control Fus. **46**, 653 (2004)
20. G.L. Majstorović, N.M. Šišović, J. Res. Phys. **36**, 1 (2012)
21. H.N. Chu, E.A. Den Hartog, A.R. Lefkow, J. Jacobs, L.W. Anderson, M.G. Lagally, J.E. Lawler, Phys. Rev. A **44**, 3796 (1991)
22. N. Goyette, W.B. Jameson, L.W. Anderson, J.E. Lawler, J. Phys. D Appl Phys. **29**, 1197 (1996)
23. U. Fantz and D. Wünderlich, *Franck-Condons Factors, Transition probabilities and radiative lifetimes for hydrogen molecules and their isotopomere* (INDC(NDS)-457 2004)
24. G. Herzberg, *in Molecular Spectra and Molecular Structure, Spectra of Diatomic Molecules*, vol. 1 (Krieger Publishing Co, Malabar, 1989)
25. I.R. Videnović, N. Konjević, M.M. Kuraica, Spectrochim. Acta B **51**, 1707 (1996)
26. M.M. Kuraica, N. Konjević, Appl. Phys. Lett. **70**, 1521 (1997)
27. H.M. Crosswhite, *The hydrogen molecule wavelength tables* (Wiley-Interscience, New York, 1972)
28. B.P. Lavrov, *Plasma Chemistry* (Energoatomizdat, Moscow, 1948)
29. I. Covacs, *in Rotational structure in the spectra of diatomic molecules* (LTD, London, 1969)
30. B.P. Lavrov, Opt. Spectrosc. **48**, 375 (1980)
31. B.P. Lavrov, M. Osiac, A.V. Pipa, J. Röpcke, Plasma source. Sci. Technol. **12**, 576 (2003)
32. G.L. Majstorović, J. Jovović, N.M. Šisović, Contrib. Plasma Phys. **57**, 282 (2017)

33. J. Jovović, G. Lj, Majstorovć. Contrib. Plasma Phys. **59**, 7 (2019)
34. L. Tomasini, A. Rousseau, G. Gousset, P. Leprince, J. Phys. D Appl. Phys. **29**, 1006 (1996)
35. G. Majstorović, M. Vasiljević, N. Šišović, Plasma Phys. Technol. **5**(3), 128 (2018)
36. S.I. Gritsinin, I.A. Kossyi, N.I. Malykh, V.G. Ral'chenko, K.F. Sergeichev, V.P. Silakov, I.A. Sychev, N.M. Tarasova, A.V. Chebotarev, J. Phys. D Appl. Phys. **31**, 2942 (1998)
37. S.A. Astashkevich, B.P. Lavrov, Opt. Spectrosc. **92**, 818 (2002)
38. M. Osiac, B.P. Lavrov, J. Röpcke, J. Quant. Spectrosc. Radiat. Transf. **74**, 471 (2002)
39. J. Yoon, M. Song, J. Han, S. Hwang, W. Chang, B. Lee, Y. Itikawa, J. Phys. Chem. Ref. Data **37**, 913 (2008)
40. G.R. Mohlmann, F.J. de Herr, Chem. Phys. Lett. **43**, 240–4 (1976)
41. A. Bogaerts, Ph. D thesis, University of Antwerp, (1996)